ACCELERATED PUBLICATION

Cholesterol-dependent phase separation in cell-derived giant plasma-membrane vesicles

Ilya LEVENTAL*, Fitzroy J. BYFIELD†, Pramit CHOWDHURY‡, Feng GAI‡, Tobias BAUMGART‡ and Paul A. JANMEY§‖[1]

*Department of Bioengineering, University of Pennsylvania, 1010 Vagelos Laboratories, 3340 Smith Walk, Philadelphia, PA 19104, U.S.A., †Institute for Medicine and Engineering, University of Pennsylvania, 1010 Vagelos Laboratories, 3340 Smith Walk, Philadelphia, PA 19104, U.S.A., ‡Department of Chemistry, University of Pennsylvania, 1010 Vagelos Laboratories, 3340 Smith Walk, Philadelphia, PA 19104, U.S.A., §Department of Physics, University of Pennsylvania, 1010 Vagelos Laboratories, 3340 Smith Walk, Philadelphia, PA 19104, U.S.A., and ‖Department of Physiology, University of Pennsylvania, 1010 Vagelos Laboratories, 3340 Smith Walk, Philadelphia, PA 19104, U.S.A.

Cell-derived GPMVs (giant plasma-membrane vesicles) enable investigation of lipid phase separation in a system with appropriate biological complexity under physiological conditions, and in the present study were used to investigate the cholesterol-dependence of domain formation and stability. The cholesterol level is directly related to the abundance of the liquid-ordered phase fraction, which is the majority phase in vesicles from untreated cells. Miscibility transition temperature depends on cholesterol and correlates strongly with the presence of detergent-insoluble membrane in cell lysates. Fluorescence correlation spectroscopy reveals two distinct diffusing populations in phase-separated cell membrane-derived vesicles whose diffusivities correspond well to diffusivities in both model systems and live cells. The results of the present study extend previous observations in purified lipid systems to the complex environment of the plasma membrane and provide insight into the effect of cholesterol on lipid phase separation and abundance.

Key words: giant plasma-membrane vesicle (GPMV), lipid raft, liquid ordered.

INTRODUCTION

Several lines of evidence, including the identification [1] and characterization [2] of detergent-resistant membrane fractions, anomalous diffusion of membrane bound tracers [3] and nanoscale aggregation of fluorescent proteins and markers [4,5], have been used to develop the hypothesis of cholesterol- and sphingolipid-enriched membrane rafts in the plasma membrane [6]. The current conception of rafts consists of transient nanoscopic domains within the bulk membrane which contain a variety of specific proteins and lipids. These domains have been proposed as platforms for the organization and concentration of signalling components [2]. Model system experiments using mixtures of synthetic lipids in monolayers [7], supported bilayers [8] and giant vesicles [9,10] have reproduced and extensively characterized liquid-phase demixing in mixtures of cholesterol and various phospholipids [11]. A consistent result across all model systems is that inclusion of cholesterol in lipid mixtures can result in liquid–liquid phase separation into an L_o (liquid-ordered) and an L_d (liquid-disordered) phase [11,12]. The L_o phase is characterized by conformational ordering resembling a crystalline/gel phase [13], but distinguished from it by a high degree of rotational and translation mobility, characteristic of the L_d phase [14]. This L_o–L_d coexistence has been proposed to be the physicochemical basis for plasma-membrane rafts, which have been postulated to be ordered phase domains.

Although model system experiments have successfully recapitulated cholesterol-dependent liquid-phase coexistence, they have offered no conclusive evidence that L_d–L_o phase immiscibility is physiologically related to cell-membrane rafts. This limitation is due, in part, to the fact that model systems cannot replicate the tremendous complexity of the plasma membrane, both in the heterogeneity of lipid species and the inclusion of membrane-associated proteins that affect the thermodynamics of lipid-mediated demixing. However, recent experiments using GPMVs (giant plasma-membrane vesicles), cell-derived liposomes that maintain the lipid [15] and protein [16] diversity of the plasma bilayer, have shown temperature-dependent liquid–liquid phase separation, similar to that observed in model systems [17]. This phase separation was found to segregate known protein and lipid markers of lipid rafts, providing a link between L_d–L_o phase separation in model systems and the lipid raft hypothesis in cellular plasma membranes. Recent experiments have suggested that GPMVs exist near miscibility critical points, and therefore that the behaviour of these complex lipid and protein mixtures can be understood by universally applicable scaling laws [18].

In the present study, we extend these studies by using fluorescence microscopy and FCS (fluorescence correlation spectroscopy) to characterize liquid–liquid phase coexistence in GPMVs and find good agreement between observations in GPMVs and purified lipid model systems with regard to the dependence of phase abundance and miscibility on the cholesterol fraction. This agreement implies that phase behaviour in simple lipid mixtures can be used to approximate domain formation in the complex environment of the plasma membrane. Additionally, we find a strong correlation between the temperature-dependent separation of a raft phase in GPMVs and the detergent-resistance

Abbreviations used: FCS, fluorescence correlation spectroscopy; GPMV, giant plasma-membrane vesicle; GUV, giant unilamellar vesicle; L_o phase, liquid-ordered phase; L_d phase, liquid-disordered phase; MBCD, methyl-β-cyclodextrin; nap, naphthopyrene; rhoPE, rhodamine 1-stearoyl 2-oleoyl phosphatidylethanolamine; T_{misc}, miscibility transition temperature.

[1] To whom correspondence should be addressed (email janmey@mail.med.upenn.edu).

of cellular membranes, suggesting that these two phenomena are related and that both are related to the existence of membrane domains in the native plasma membrane.

EXPERIMENTAL

GPMVs were isolated after chemically inducing cell blebbing with 25 mM paraformaldehyde and 2 mM DTT (dithiothreitol) in calcium-containing buffer [150 mM NaCl, 10 mM Hepes and 2 mM $CaCl_2$ (pH 7.4)] for 1 h at 37 °C as previously described [17], and labelled with rhoPE (rhodamine 1-stearoyl 2-oleoyl phosphatidylethanolamine; Avanti) and/or nap (naphthopyrene; Sigma) by incubation at room temperature (23 °C) for 15 min with 2.5 μg/ml rhoPE and/or 10 μg/ml nap. A chamber was created by making a square of silicon sealant (Dow Corning) on a BSA-coated coverslip, into the middle of which 20 μl of labelled GPMV suspension was deposited, followed by sealing of the chamber with another coverslip. The fluorescence of the vesicles was visualized using an inverted microscope (Leica) equipped with appropriate filter sets. The temperature was controlled using a Peltier temperature control stage (TS-4; Physitemp) at 10 °C, unless otherwise stated. The percentage surface area covered by the L_d phase was quantified by calculating the surface area of the spherical cap (SA_{cap}) covered by the rhoPE-rich (bright) phase using the relationship (eqn 1):

$$SA_{cap} = 2\pi \times r_{vesicle} \times h_{cap} \quad (1)$$

where h_{cap} is the height of the spherical cap and equivalent to (eqn 2):

$$h_{cap} = r_{vesicle} - \sqrt{{r_{vesicle}}^2 - {r_{cap}}^2} \quad (2)$$

if L_d is the minority phase and (eqn 3),

$$h_{cap} = r_{vesicle} + \sqrt{{r_{vesicle}}^2 - {r_{cap}}^2} \quad (3)$$

if L_d is the majority phase.

$r_{vesicle}$ and r_{cap} are the radii of the vesicle and rhoPE-rich cap respectively, and were measured using ImageJ software.

FCS was performed with a confocal microscope on GPMVs as previously described for GUVs (giant unilamellar vesicles) [19,20]. Detergent-resistant membranes were isolated on a discontinuous sucrose gradient as described previously [21]. Purification and quantification of membrane lipids were performed in accordance with previously published protocols [22,23]. Further experimental details are available in the Supplementary material (at http://www.biochemj.org/bj/424/bj4240163add.htm).

RESULTS AND DISCUSSION

GPMVs derived from NIH 3T3 fibroblasts were stained with rhoPE (disordered-phase tracer), and observed by fluorescence microscopy to quantify the relative abundance of L_d and L_o phases (the L_o phase is also referred to as the 'raft phase' because it enriches for raft components [17]). The results in Figure 1 show that more than 70 % of the surface area of vesicles derived from untreated cells is composed of the raft phase, suggesting a continuous ordered bilayer in which disordered domains exist as inclusions [imaging performed at 10 °C unless otherwise stated, although phase abundances were temperature-independent over a wide range (10–24 °C; Supplementary Figure S1 at http://www.biochemj.org/bj/424/bj4240163add.htm)]. This finding is inconsistent with the concept of liquid-ordered domains as isolated and scarce lipid rafts, instead suggesting the possibility of a plasma membrane existing as a majority liquid-ordered continuum interrupted by disordered domains. The idea of a percolating raft phase is consistent with previous measurements of diffusivity of raft and non-raft protein and lipid markers [24], electron-spin resonance in live cells [25] and single-cell detergent extractions [26].

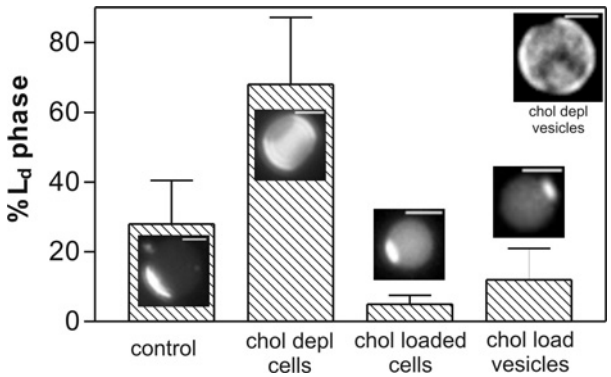

Figure 1 Fluorescence images and quantification of the L_d (non-raft) phase fraction in GPMVs (stained with rhoPE to label the L_d phase) as a function of cholesterol modulation

The cholesterol level relates inversely to the abundance of the L_d phase in GPMVs and the L_o phase is the majority phase in vesicles from untreated cells. Ribbon-like gel-phase domains are observed when cholesterol is entirely depleted by direct treatment of GPMVs. Values are means + S.D. from > 35 vesicles per condition. Scale bars = 5 μm. chol, cholesterol; depl, depleted.

Detergent-resistant membrane fractions, which formed the original basis for the raft hypothesis, are enriched in cholesterol, suggesting that lipid rafts are liquid-ordered membrane structures enriched in, and possibly dependent on, the presence of cholesterol. We modulated cholesterol levels in cells prior to GPMV isolation, and in GPMVs isolated from untreated cells, to determine whether cholesterol affects the abundance and coexistence of the two liquid phases. Depletion of cellular cholesterol by treatment with 5 mM MBCD (methyl-β-cyclodextrin) decreased the cholesterol molar fraction by more than 20 % in the derived GPMVs, and resulted in significant changes to the relative abundance of the phases, more than doubling the relative abundance of the disordered, non-raft, phase from 28 % to more than 65 % of the surface area (Figure 1). Inversely, loading cells with cholesterol by treatment with cholesterol-saturated MBCD (decreasing the GPMV phospholipid/cholesterol ratio from 1:1 to 1:0.8) led to a near disappearance of the L_d phase, from 28 % to 5 % surface area, causing these GPMVs to appear nearly dark with very small bright disordered patches. Similar results were observed when GPMVs were cholesterol-loaded after isolation from untreated cells.

Although MBCD depletion of plasma membrane cholesterol strongly affected the phase abundance of derived GPMVs, this technique was unable to deplete cholesterol below $\sim$ 35 mol % (Supplementary Figure S2 at http://www.BiochemJ.org/bj/424/bj4240163add.htm). This limitation was overcome by direct MBCD treatment of vesicles following their isolation from cells, which resulted in non-circular, jagged and ribbon-like domains (Figure 1) similar in morphology to gel-phase domains observed in cholesterol-free GUVs where demixing was the consequence of acyl chain length differences between the component phospholipids [20].

These cholesterol modulation data are consistent with purified lipid experiments that have shown cholesterol-dependent

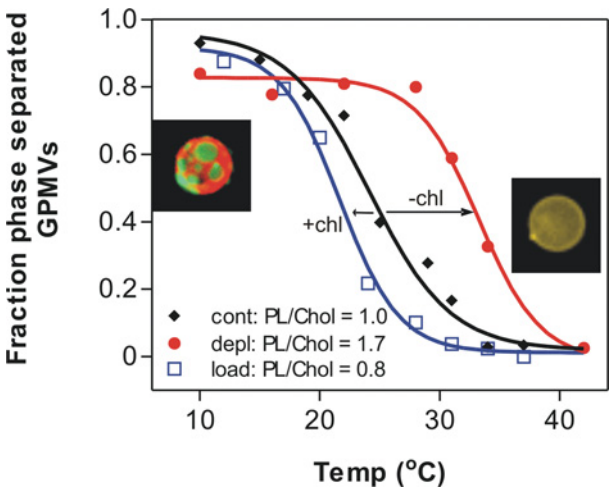

Figure 2 Temperature-dependence of phase separation in GPMVs isolated from untreated cells (black), cholesterol-depleted cells (red circles) and cholesterol-loaded cells (blue squares)

Pictures are superpositions of red and green images from epifluorescence micrographs of GPMVs prepared from untreated cells stained with rhoPE (L_d, red) and nap (L_o, green) at 10 °C (left-hand side, phase-separated) and 37 °C (right-hand side, homogeneous). cont, control; chl/chol, cholesterol; depl, depleted; PL, phospholipid.

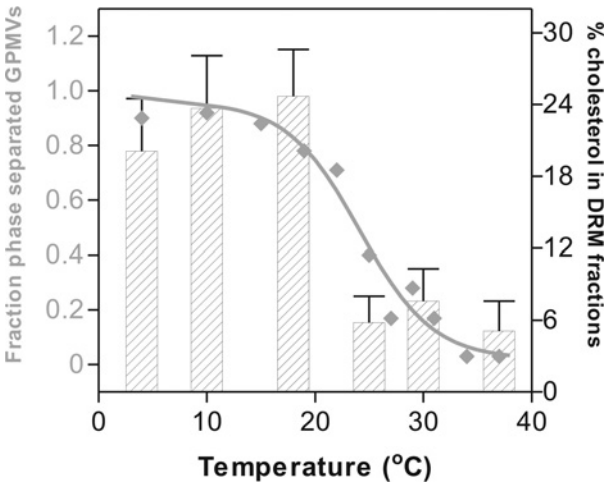

Figure 3 Correlation between the temperature-dependence of phase separation of GPMVs (diamond points, line is a sigmoidal fit) and the abundance of detergent-resistant membranes (detergent solubilization performed at the indicated temperatures) as quantified by the percentage of cholesterol in the detergent-resistant fractions (striped bars)

Values are means ± S.D. Low temperatures, which induce GPMV phase separation, also induce Triton-resistant membrane fractions as quantified by the presence of cholesterol in low-density fractions (fractions 1–3 for all temperatures, except 10 °C where detergent-resistance membranes were in fractions 1–6; see Supplementary Figure S3 at http://www.BiochemJ.org/bj/424/bj4240163add.htm). DRM, detergent-resistant membrane.

formation of a L_o phase, and the abolition or reduction of that phase when cholesterol was depleted [10,27]. The induction of a non-fluid gel phase by wholesale depletion of cholesterol is consistent with liquid/gel phase separation in GUVs lacking cholesterol [20], as well as measurements in cholesterol-depleted live cells [28] and observations of viral lipid extracts [29].

In addition to phase abundance, the cholesterol molar fraction affects phase separation in numerous simplified lipid model systems [11], prompting the hypothesis that the same effect might be observed in the complex lipid and protein mixture of GPMVs. Cellular cholesterol levels were manipulated as above, and the temperature-dependent phase separation of GPMVs derived from those cells was measured. Loading cells with cholesterol (~ 20 % decrease in [phospholipid]/[cholesterol]) decreased the average miscibility transition temperature (T_{misc}) from 24 to 21 °C, whereas depleting cellular cholesterol increased T_{misc} to 32 °C. Cholesterol depletion also produced a significant fraction (15 %) of microscopically phase-separated vesicles at 37 °C, suggesting the possibility of cholesterol-dependent phase separation in complex membranes at physiological conditions (Figure 2). This observation corresponds well to phase separation induced by cholesterol depletion of live cells at physiological temperatures [26]. Additionally, the cholesterol molar fraction dependence of T_{misc} (Figure 2) closely resembles the same dependence measured in model liposomes [27]. This agreement is particularly striking since not only the trends, but also the absolute values of the transition temperatures, are similar for three-component GUVs and the much more complex cell-derived vesicles considered here, suggesting that findings in purified lipid systems can be extended to multi-component, cell-derived protein–lipid mixtures.

The findings presented above show that phase abundance and miscibility as a function of cholesterol in GPMVs correspond well to the same properties observed in simple systems. At the opposite extreme of complexity from purified lipid models of membrane rafts are the detergent-resistant membrane fractions that suggest the existence of biochemically distinct membrane domains in whole-cell lysates. To determine the relationship between fluid-phase coexistence in GPMVs and the presence of a low-density membrane fraction in detergent-lysed cells, the temperature-dependence of these two distinct membrane phenomena was investigated by also performing sucrose-gradient fractionation of cell membranes at different temperatures. The temperature profile of microscopically observable phase coexistence in GPMVs from untreated cells followed a relatively abrupt transition from entirely phase-separated to microscopically uniform vesicles between 20 and 25 °C. The temperature-dependent abundance of the mass of cholesterol in detergent-resistant membrane fractions yielded a very similar temperature profile, with the detergent-resistant fractions making up 20–25 % (w/w) of the total cholesterol below the phase-transition temperature of the GPMVs, but <10 % above (Figure 3 and Supplementary Figure S3 at http://www.BiochemJ.org/bj/424/bj4240163add.htm). The temperature-dependent presence of a detergent-resistant component was confirmed by quantifying the sucrose-gradient distribution of a protein reported to partition to detergent-insoluble rafts. Below 20 °C, > 50 % of Alexa Fluor® 488-labelled CTB (fluorescently labelled cholera toxin B) was recovered in low-density fractions, whereas <15 % was detergent-resistant above this average GPMV phase-separation temperature (Supplementary Figure S4 at http://www.BiochemJ.org/bj/424/bj4240163add.htm).

Although the requirement for low temperature and detergent treatment has led to intense scrutiny regarding the physiological relevance of detergent-resistant membranes [30], we find a strong correlation between detergent-resistance and GPMV phase separation. This result suggests that detergent-insolubility and the existence of a separated ordered phase in complex mixtures are related, and that both are related to membrane rafts. These results confirm findings from detergent extractions of mixed lipid vesicles [9,31] and GPMVs [32], and argue against the artefactual induction of liquid-phase coexistence by detergent as the sole mechanism for raft formation. Although neither microscopically observable phase separation nor detergent-resistance (without cyclodextrin treatment) was observed in our experiments at physiological temperature (37 °C), the

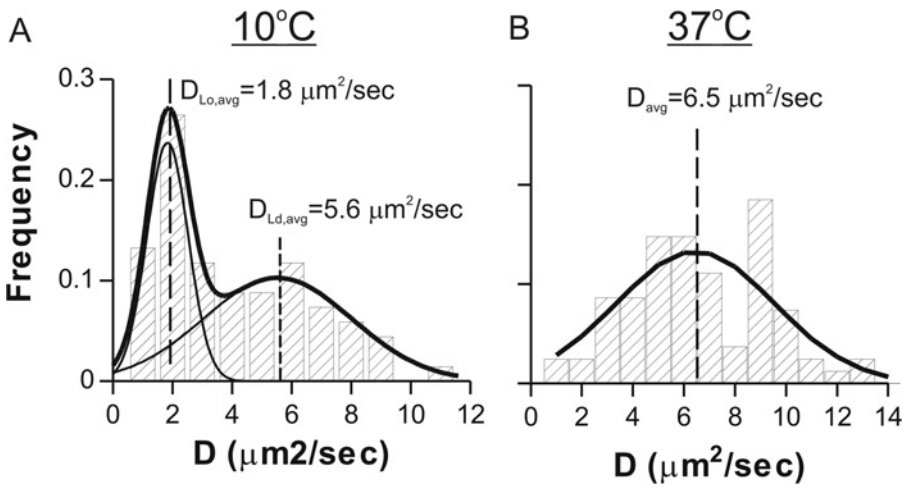

Figure 4 Histograms of diffusion coefficients obtained by FCS of rhoPE diffusing in (A) phase-separated vesicles at 10 °C and (B) microscopically uniform vesicles at 37 °C

Diffusion coefficients were calculated by fitting autocorrelation data to a two-component two-dimensional diffusion equation (for experimental details see the Supplementary Experimental section at http://www.BiochemJ.org/bj/424/bj4240163add.htm). These results show a single diffusing population of tracers in uniform vesicles and two distinct populations in phase-separated vesicles [bold lines are Gaussian fits to all data and thin lines in (**A**) show the component Gaussians]. Histograms are from > 70 measurements on seven to nine vesicles per condition.

phase separation in GPMVs and detergent-resistance of certain membrane fractions might occur due to the coalescence of underlying nanoscopic assemblies of raft lipids and proteins, recently proposed thermodynamically [18] and experimentally [33], that are neither microscopically observable nor detergent-insoluble at 37 °C.

One of the distinguishing characteristics of ordered compared with disordered fluid phases in model lipid systems is a difference in translational and rotational diffusivity [13]; lipid and protein diffusivity are major determinants of the cellular distribution and corresponding functions of plasma-membrane components. Lipid diffusivity was quantified in both phase-separated and uniform GPMVs by FCS on fluorescent tracer lipids incorporated into the vesicles. At a temperature at which GPMVs separate into two liquid phases (10 °C), we observed two distinct populations of diffusion coefficients obtained from fits to autocorrelation data (Figure 4). The histogram fitted to normal distribution yield average diffusivities of 1.8 and 5.6 $\mu m^2/s$. The correlation data at 37 °C suggest a single population of diffusion coefficients with a mean value approximately equivalent to that of the faster diffusing component at 10 °C (Figure 4b). These results agree well with previous measurements in both cells and model systems. The 3-fold difference in lateral mobility between the two phases is almost exactly the same as was measured by fluorescence recovery in DMPC (dimyristoyl phosphatidylcholine)-cholesterol bilayers at physiological temperature [13]. The diffusion coefficients measured in L_o and L_d phases are very close to the diffusion coefficients measured here, strongly suggesting that the 1.8 $\mu m^2/s$ component corresponds to the L_o (raft) phase of GPMVs, whereas the faster component is likely to be the disordered phase. The diffusivity differences and magnitudes measured here correspond very well to those measured by FCS for L_d and L_o phase markers in raft-composition GUVs [19], as well as to small-scale diffusivities previously measured in live cells by optical tweezers [34], underlining the agreement not just in phase separation, but also in the properties of those phases, among live cells, GPMVs and purified lipid systems.

The results of the present study demonstrate that complex multi-component lipid and protein membranes can exhibit similar phase behaviour as simple three-component model membranes with respect to abundance, diffusivity and phase separation. Our findings also suggest that this behaviour is related to the detergent-resistance of biological membranes, thereby relating biochemical and biophysical descriptions of membrane rafts and suggesting an important role for GPMVs as an intermediate lipid raft model system combining the complexity of the biological membrane with the observable phase separation and experimental simplicity of purified lipid mixtures.

AUTHOR CONTRIBUTION

Ilya Levental designed and performed experiments and wrote the paper. Fitzroy Byfield and Pramit Chowdhury performed experiments. Feng Gai and Tobias Baumgart designed experiments. Paul Janmey designed experiments and wrote the paper.

FUNDING

This work was supported by the National Science Foundation [grant number MRSEC 05-20020]; and the National Institutes of Health [grant numbers AR38910, R21AI073409].

REFERENCES

1 Brown, D. A. and Rose, J. K. (1992) Sorting of GPI-anchored proteins to glycolipid-enriched membrane subdomains during transport to the apical cell surface. Cell **68**, 533–544
2 Simons, K. and Toomre, D. (2000) Lipid rafts and signal transduction. Nat. Rev. Mol. Cell Biol. **1**, 31–39
3 Schutz, G. J., Kada, G., Pastushenko, V. P. and Schindler, H. (2000) Properties of lipid microdomains in a muscle cell membrane visualized by single molecule microscopy. EMBO J. **19**, 892–901
4 Varma, R. and Mayor, S. (1998) GPI-anchored proteins are organized in submicron domains at the cell surface. Nature **394**, 798–801
5 Harder, T., Scheiffele, P., Verkade, P. and Simons, K. (1998) Lipid domain structure of the plasma membrane revealed by patching of membrane components. J. Cell Biol. **141**, 929–942
6 Simons, K. and Ikonen, E. (1997) Functional rafts in cell membranes. Nature **387**, 569–572
7 Keller, S. L., Anderson, T. G. and McConnell, H. M. (2000) Miscibility critical pressures in monolayers of ternary lipid mixtures. Biophys. J. **79**, 2033–2042

8 Dietrich, C., Volovyk, Z. N., Levi, M., Thompson, N. L. and Jacobson, K. (2001) Partitioning of Thy-1, GM1, and cross-linked phospholipid analogs into lipid rafts reconstituted in supported model membrane monolayers. Proc. Natl. Acad. Sci. U.S.A. **98**, 10642–10647
9 Dietrich, C., Bagatolli, L. A., Volovyk, Z. N., Thompson, N. L., Levi, M., Jacobson, K. and Gratton, E. (2001) Lipid rafts reconstituted in model membranes. Biophys. J. **80**, 1417–1428
10 Veatch, S. L. and Keller, S. L. (2002) Organization in lipid membranes containing cholesterol. Phys. Rev. Lett. **89**, 268101–268105
11 McConnell, H. M. and Vrljic, M. (2003) Liquid-liquid immiscibility in membranes. Annu. Rev. Biophys. Biomol. Struct. **32**, 469–492
12 Simons, K. and Vaz, W. L. (2004) Model systems, lipid rafts, and cell membranes. Annu. Rev. Biophys. Biomol. Struct. **33**, 269–295
13 Almeida, P. F., Vaz, W. L. and Thompson, T. E. (1993) Percolation and diffusion in three-component lipid bilayers: effect of cholesterol on an equimolar mixture of two phosphatidylcholines. Biophys. J. **64**, 399–412
14 Gally, H. U., Seelig, A. and Seelig, J. (1976) Cholesterol-induced rod-like motion of fatty acyl chains in lipid bilayers a deuterium magnetic resonance study. Hoppe Seylers Z. Physiol. Chem. **357**, 1447–1450
15 Fridriksson, E. K., Shipkova, P. A., Sheets, E. D., Holowka, D., Baird, B. and McLafferty, F. W. (1999) Quantitative analysis of phospholipids in functionally important membrane domains from RBL-2H3 mast cells using tandem high-resolution mass spectrometry. Biochemistry **38**, 8056–8063
16 Scott, R. E., Perkins, R. G., Zschunke, M. A., Hoerl, B. J. and Maercklein, P. B. (1979) Plasma membrane vesiculation in 3T3 and SV3T3 cells. I. Morphological and biochemical characterization. J. Cell Sci. **35**, 229–243
17 Baumgart, T., Hammond, A. T., Sengupta, P., Hess, S. T., Holowka, D. A., Baird, B. A. and Webb, W. W. (2007) Large-scale fluid/fluid phase separation of proteins and lipids in giant plasma membrane vesicles. Proc. Natl. Acad. Sci. U.S.A. **104**, 3165–3170
18 Veatch, S. L., Cicuta, P., Sengupta, P., Honerkamp-Smith, A., Holowka, D. and Baird, B. (2008) Critical fluctuations in plasma membrane vesicles. ACS Chem. Biol. **3**, 287–293
19 Bacia, K., Scherfeld, D., Kahya, N. and Schwille, P. (2004) Fluorescence correlation spectroscopy relates rafts in model and native membranes. Biophys. J. **87**, 1034–1043
20 Korlach, J., Schwille, P., Webb, W. W. and Feigenson, G. W. (1999) Characterization of lipid bilayer phases by confocal microscopy and fluorescence correlation spectroscopy. Proc. Natl. Acad. Sci. U.S.A. **96**, 8461–8466
21 Lingwood, D. and Simons, K. (2007) Detergent resistance as a tool in membrane research. Nat. Protoc. **2**, 2159–2165
22 Bligh, E. G. and Dyer, W. J. (1959) A rapid method of total lipid extraction and purification. Can. J. Biochem. Physiol. **37**, 911–917
23 Kates, M. (1986) Techniques of Lipidology, Elsevier Science Publishers B.V., Amsterdam
24 Meder, D., Moreno, M. J., Verkade, P., Vaz, W. L. and Simons, K. (2006) Phase coexistence and connectivity in the apical membrane of polarized epithelial cells. Proc. Natl. Acad. Sci. U.S.A. **103**, 329–334
25 Swamy, M. J., Ciani, L., Ge, M., Smith, A. K., Holowka, D., Baird, B. and Freed, J. H. (2006) Coexisting domains in the plasma membranes of live cells characterized by spin-label ESR spectroscopy. Biophys. J. **90**, 4452–4465
26 Hao, M., Mukherjee, S. and Maxfield, F. R. (2001) Cholesterol depletion induces large scale domain segregation in living cell membranes. Proc. Natl. Acad. Sci. U.S.A. **98**, 13072–13077
27 Veatch, S. L. and Keller, S. L. (2003) Separation of liquid phases in giant vesicles of ternary mixtures of phospholipids and cholesterol. Biophys. J. **85**, 3074–3083
28 Nishimura, S. Y., Vrljic, M., Klein, L. O., McConnell, H. M. and Moerner, W. E. (2006) Cholesterol depletion induces solid-like regions in the plasma membrane. Biophys. J. **90**, 927–938
29 Polozov, I. V., Bezrukov, L., Gawrisch, K. and Zimmerberg, J. (2008) Progressive ordering with decreasing temperature of the phospholipids of influenza virus. Nat. Chem. Biol. **4**, 248–255
30 Lichtenberg, D., Goni, F. M. and Heerklotz, H. (2005) Detergent-resistant membranes should not be identified with membrane rafts. Trends Biochem. Sci. **30**, 430–436
31 Ahmed, S. N., Brown, D. A. and London, E. (1997) On the origin of sphingolipid/cholesterol-rich detergent-insoluble cell membranes: physiological concentrations of cholesterol and sphingolipid induce formation of a detergent-insoluble, liquid-ordered lipid phase in model membranes. Biochemistry **36**, 10944–10953
32 Sengupta, P., Hammond, A., Holowka, D. and Baird, B. (2008) Structural determinants for partitioning of lipids and proteins between coexisting fluid phases in giant plasma membrane vesicles. Biochim. Biophys. Acta **1778**, 20–32
33 Lingwood, D., Ries, J., Schwille, P. and Simons, K. (2008) Plasma membranes are poised for activation of raft phase coalescence at physiological temperature. Proc. Natl. Acad. Sci. U.S.A. **105**, 10005–10010
34 Pralle, A., Keller, P., Florin, E. L., Simons, K. and Horber, J. K. H. (2000) Sphingolipid-cholesterol rafts diffuse as small entities in the plasma membrane of mammalian cells. J. Cell Biol. **148**, 997–1008

Received 17 August 2009/28 September 2009; accepted 7 October 2009
Published as BJ Immediate Publication 7 October 2009, doi:10.1042/BJ20091283

Biochem. J. (2009) **424**, 163–167 (Printed in Great Britain) doi:10.1042/BJ20091283

online data

SUPPLEMENTARY ONLINE DATA

Cholesterol-dependent phase separation in cell-derived giant plasma-membrane vesicles

Ilya LEVENTAL*, Fitzroy J. BYFIELD†, Pramit CHOWDHURY‡, Feng GAI‡, Tobias BAUMGART‡ and Paul A. JANMEY§‖[1]

*Department of Bioengineering, University of Pennsylvania, 1010 Vagelos Laboratories, 3340 Smith Walk, Philadelphia, PA 19104, U.S.A., †Institute for Medicine and Engineering, University of Pennsylvania, 1010 Vagelos Laboratories, 3340 Smith Walk, Philadelphia, PA 19104, U.S.A., ‡Department of Chemistry, University of Pennsylvania, 1010 Vagelos Laboratories, 3340 Smith Walk, Philadelphia, PA 19104, U.S.A., §Department of Physics, University of Pennsylvania, 1010 Vagelos Laboratories, 3340 Smith Walk, Philadelphia, PA 19104, U.S.A., and ‖Department of Physiology, University of Pennsylvania, 1010 Vagelos Laboratories, 3340 Smith Walk, Philadelphia, PA 19104, U.S.A.

EXPERIMENTAL

Cell culture and treatment

NIH 3T3 fibroblasts were cultured at 37 °C in 5 % CO_2 in DMEM (Dulbecco's modified Eagle's medium; Gibco) supplemented with 10 % (v/v) calf serum (Gibco). For cholesterol depletion, cells at 70 % confluence were treated with 5 mM MBCD dissolved in serum-free DMEM for 1 h at 37 °C. For cholesterol loading, the treatment was the same except the MBCD was pre-loaded with cholesterol by overnight incubation with 160 μg of cholesterol [$\sim$ 2.5 % (w/w); Avanti].

Image analysis

Image analysis was performed as described in the Experimental section of the main text.

Phospholipid/cholesterol quantification

Cells were grown to 70 % confluence in T150 flasks (Corning), treated with cholesterol-free or cholesterol-loaded MBCD, and GPMVs were isolated as described in the main text (the large number of cells was necessary to get a detectable signal from the phosphate assay). The vesicle suspension was then extracted using the Bligh and Dyer method [1] with 3.75 ml of chloroform/methanol (1:2) per 1 ml of suspension overnight at room temperature. Phase separation was induced by adding 1.25 ml of double-distilled H_2O and 1.25 ml of chloroform. The samples were then centrifuged for 10 min at 2000 ***g***; the top (aqueous) phase was aspirated, and the bottom (organic, lipid-rich) phase was saved. A portion (10 %) of the resulting organic phase was analysed for cholesterol concentration as follows: the extracted lipid solution was dried under nitrogen, rehydrated with water, vortex-mixed briefly and then sonicated for 30 min at room temperature to produce small vesicles composed of the extracted lipid components. These vesicles were then analysed for their cholesterol content using a fluorimetric enzymatic kit (Amplex Red Cholesterol Assay Kit, Invitrogen) following the manufacturer's protocol. The remaining organic phase was used to quantify the phospholipid concentration using a colorimetric inorganic phosphate assay [2]. The results from these assays were then combined to determine the relative molar abundance of cholesterol and phospholipids, with the simplifying assumption that there was one phosphate per phospholipid.

FCS of GPMVs

The excitation source at 514.5 nm was derived from the laser lines of an Ar^+ laser (Spectra-Physics), which was brought to focus in the sample solution by a microscope objective [Nikon 63×, NA (numerical aperture) 1.3, oil-immersion]. The emission was collected by the same objective and was separated from the excitation light by a dichroic mirror. The confocal volume was defined by a 50 μm pinhole. Photon counting in real-time was achieved by a SPCM-AQR-16 avalanche photodiode (PerkinElmer), and a Flex 03-LQ-01 correlator card

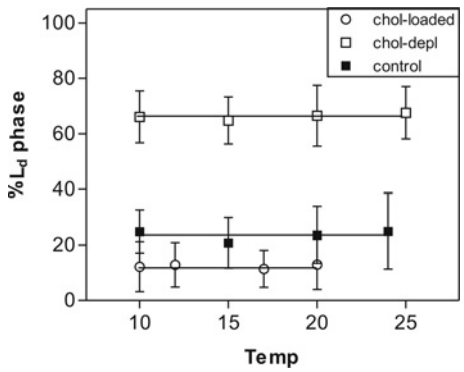

Figure S1 Temperature-independent phase abundances

Quantification of relative surface area covered by the L_d phase in vesicles as a function of temperature. Error bars are S.D. from 20 vesicles measured per condition; results are representative of three different experiments and clearly show the lack of effect of temperature on the L_d phase fraction. chol, cholesterol: depl, depleted.

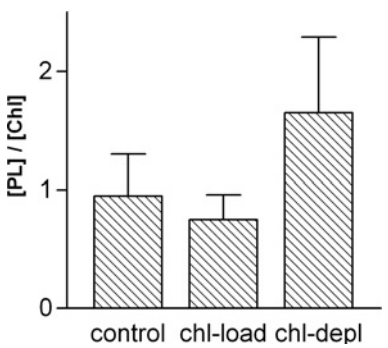

Figure S2 Phospholipid/cholesterol quantification

Ratio of the concentration of phospholipids to cholesterol in GPMVs derived from cells with the indicated treatments. Error bars are S.D. from three separate experiments. The average concentrations of the components were (phospholipid/cholesterol): control (655 μM/623 μM); cholesterol-loaded (463 μM/574 μM); cholesterol-depleted (993 μM/558 μM). chl, cholesterol; depl, depleted; PL, phospholipid.

[1] To whom correspondence should be addressed (email janmey@mail.med.upenn.edu).

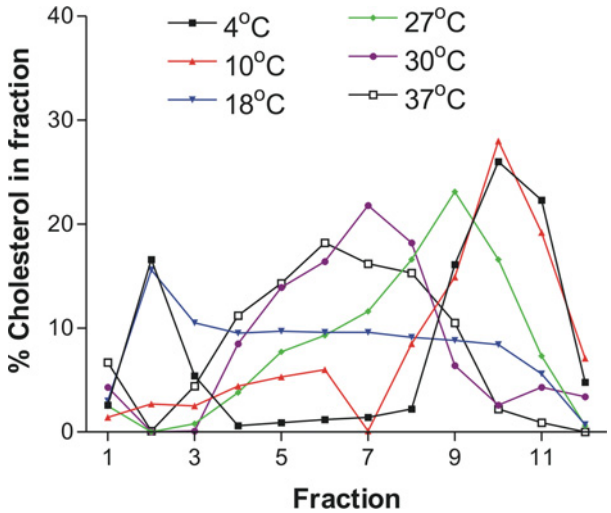

Figure S3 Triton-extracted cholesterol distribution in sucrose gradients

Temperature-dependent percentage mass of cholesterol in the fractions of a sucrose step gradient where the first fraction is the lightest and the 12th is the densest. Representative profiles from three trials are shown for 4 °C (black squares), 10 °C (red diamonds), 18 °C (blue triangles), 27 °C (green diamonds), 30 °C (purple circles) and 37 °C (black open squares). Low temperatures, at which GPMVs phase-separate, induce the presence of cholesterol in Triton-resistant fractions (fractions 1–3 for all temperatures except 10 °C which was fractions 1–6). These fractions lack cholesterol at temperatures above 27 °C. Intermediate temperatures (namely 18 °C) where both phase-separated and uniform vesicles are present, have cholesterol in almost all fractions, suggesting a continuum of detergent-resistant and labile components.

(http://Correlator.com) was used to control the data collection as well as the subsequent autocorrelation analysis for the FCS measurements. The vesicles were labelled as described above, with the exception that the final labelling concentration was 1 nM rhoPE (this labelling concentration was an important parameter for good correlation). The confocal volume was calibrated by measuring the correlation arising from the free diffusion of a known dye solution (rhodamine 6G, $D_T = 2.8 \times 10^{-6}$ cm^2/s). GPMVs were then placed in a chamber (as above), located using phase contrast and positioned such that the middle of the vesicle was superimposed on the focal laser spot. The focus was then adjusted such that the laser spot was focused on to the top of the membrane (measurements taken from the bottom and side membranes did not yield significantly different results). The laser power at the back port of the microscope was kept low enough to minimize photobleaching of the fluorescent reporters and the fluorescence bursts were detected for 30 s/measurement. In total, seven to ten vesicles per condition were measured at various focal planes with 15–20 measurements/vesicle. Repeat measurements taken at the same spot were quite reproducible and gave nearly identical results.

Correlation curves [$G(\tau)$ against τ] were fitted from $\tau = 1 \times 10^{-4}$ to 5 s with the following two-component two-dimensional diffusion equation, where one of the components was the vesicle-unincorporated dye diffusing much faster than those in the vesicle ($\tau_{free} \sim$ 150–400 μm^2/s):

$$G(\tau) = \frac{1}{N}\left[(1 - f_{free})\left(1 + \frac{\tau}{\tau_D}\right)^{-1} + f_{free}\left(1 + \frac{\tau}{\tau_{D,free}}\right)^{-1}\right]$$

where N is the average number of fluorescent molecules in the confocal volume, τ_D is the diffusion time of the membrane-bound component, and f_{free} is the fraction of unincorporated dye molecules. The diffusion coefficients can be further defined as:

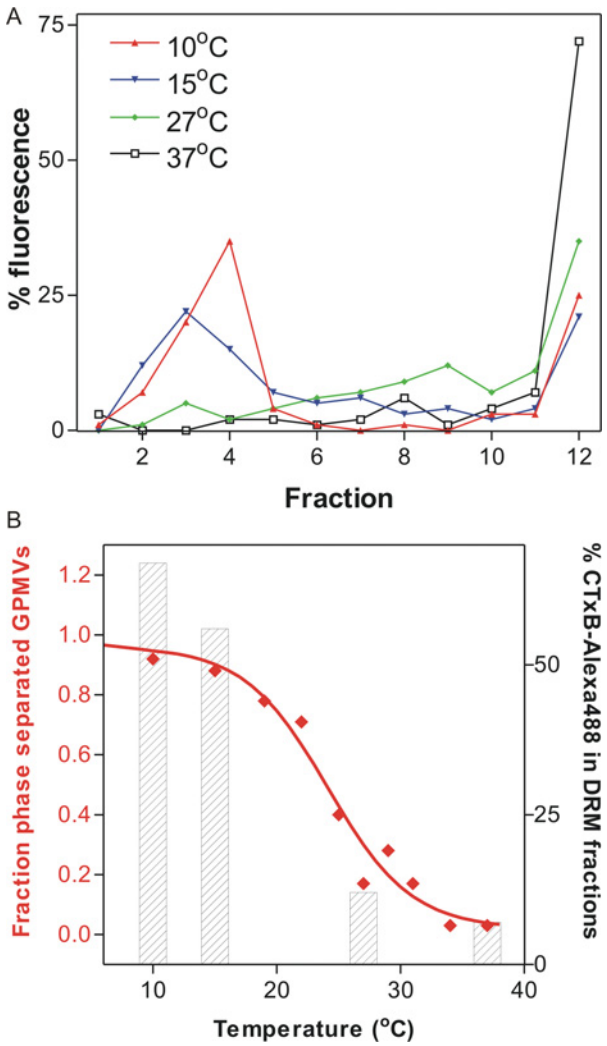

Figure S4 Correlation between Triton-insoluble Alexa Fluor® 488–CTB and GPMV phase-separation temperature

(**A**) Temperature-dependent fluorescence of the G_{M1}-binding Alexa Fluor® 488–CTB in the fractions of a sucrose step gradient where the first fraction is the lightest and the 12th is the densest. Profiles are shown for 10 °C (red triangles), 15 °C (blue triangles), 27 °C (green circles) and 37 °C (black squares). Temperatures below the average phase-separation temperature of untreated GPMVs (~ 23 °C) clearly show the presence of detergent-resistant membranes by the high fluorescence of low-density fractions, in contrast with the samples above the GPMV phase-transition temperature, which only show Alexa Fluor® 488–CTB fluorescence in high-density, detergent-solubilized fractions. (**B**) Detergent-resistant membrane (DRM) abundance, as quantified by the percentage of Alexa Fluor® 488-labelled CTB in the light fractions (1–5), and its correlation with the phase separation of GPMVs at different temperatures (compare with a similar correlation in Figure 3 of the main text).

$$D_T = \frac{r_0^2}{4\tau_D}$$

where r_0 is the radius of the confocal volume defined by the free dye calibration (for these experiments = 0.33 μm). A small number of curves at 10 °C (< 5 %) were not fitted well by the two-component model and required a three-component fit and these were interpreted as capturing tracers in both phases during the 30 s of acquisition of the FCS data (in addition to the free dye).

Membrane-bound components were differentiated from the unincorporated, freely diffusing fluorescent tracers by the magnitude of measured diffusivity (~ 100× slower for the membrane-bound dye).

Detergent-resistant membrane fraction quantification

NIH 3T3 fibroblasts were grown to 70 % confluence in 10 cm dishes (Becton Dickinson). The cells were then harvested by trypsinization, and the trypsin was inactivated using soya bean trypsin inhibitor (Sigma). The cells were then washed twice in TNE buffer [25 mM Tris/HCl, 150 mM NaCl and 5 mM EDTA (pH 7.4)]. After the second wash, the cells were resuspended in TNE supplemented with 1 % Triton X-100 (Sigma) and protease inhibitor cocktail (Sigma; 10 μl per ml of lysate) and lysed for 30 min in a temperature-controlled water bath. Following lysis, the cells were homogenized while immersed in a temperature-controlled bath by shearing through a 25-gauge needle (20 strokes). Lysate (1 ml) was then mixed with 2 ml of 56 % sucrose to make 3 ml of 40 % sucrose lysate solution, which was overlaid with 7 ml of 35 % sucrose, followed by 2 ml of 5 % sucrose. This gradient was then centrifuged at 39000 rev./min for 18 h. Fractions (1 ml each) were then analysed for their cholesterol content as described above. Detergent-resistant fractions were defined as fractions 1–3 from the top of the column in all samples except for those extracted at 10 °C. At this temperature (as well as at 18 °C) a significant amount of cholesterol was found in the intermediate fractions 4–7 (Supplementary Figure S4), probably reflecting the presence of a transition state between detergent-labile and detergent-resistant membranes. For detergent-resistant membrane quantification of the 10 °C samples, the detergent-resistant fractions were defined as those lighter than the fraction in which no cholesterol was observed (fractions 6, 7 and 7 for the three 10 °C repeats, fraction 7 in the sample shown in Supplementary Figure S4).

There is some evidence that cholesterol may be enriched in the detergent-resistant fractions [3], which suggests that estimating detergent-resistant membrane fraction by cholesterol quantification may overstate the abundance of the detergent-resistant phase. This is not a significant concern because not only would this error be systematic and not affect the results shown in Figure 3 of the main text, but also a recent study suggests that the DRM phase may have an equal cholesterol concentration to that of the detergent-labile phase [4].

To study the temperature-dependent detergent-resistance of the G_{M1}-binding pentameric B subunit of the cholera toxin (CTB, a canonical raft marker), cells were incubated prior to Triton lysis with 50 μg/ml Alexa Fluor® 594-labelled CTB (Molecular Probes) for 1 h at 4 °C. Following lysis and fractionation, the fluorescence of each fraction was measured using an LS-5B spectrofluorimeter (PerkinElmer). The presence of CTB was clearly segregated between a detergent-resistant peak (fractions 3–4) and a detergent-labile peak (fraction 12), so the detergent-resistant fractions were defined as fractions 1–5.

The data in Supplementary Figure S4 clearly confirm the data presented in Figure 3 of the main text and Supplementary Figure S3, namely the presence of detergent-resistant components below the phase-transition temperature of GPMVs.

Received 17 August 2009/28 September 2009; accepted 7 October 2009
Published as BJ Immediate Publication 7 October 2009, doi:10.1042/BJ20091283

REFERENCES

1 Bligh, E. G. and Dyer, W. J. (1959) A rapid method of total lipid extraction and purification. Can. J. Biochem. Physiol. **37**, 911–917
2 Kates, M. (1986) Techniques of Lipidology. Elsevier Science Publishers B.V., Amsterdam
3 Simons, K. and Ikonen, E. (1997) Functional rafts in cell membranes. Nature **387**, 569–572
4 Ayuyan, A. G. and Cohen, F. S. (2007) Raft composition at physiological temperature and pH in the absence of detergents. Biophys. J. **94**, 2654–2666